Available online at www.sciencedirect.com
SCIENCE DIRECT®
Journal of Pharmaceutical and Biomedical Analysis 37 (2005) 351–358
JOURNAL OF PHARMACEUTICAL AND BIOMEDICAL ANALYSIS
www.elsevier.com/locate/jpba

In vitro metabolism of a new oxazolidinedione hypoglycemic agent utilizing liver microsomes and recombinant human cytochrome P450 enzymes

Arun K. Agrawal[a,*], Cornelis E.C.A. Hop[a,1], Jianmei Pang[a], Maria V. Silva Elipe[a], Ranjit C. Desai[b], Kwan H. Leung[a], Ronald B. Franklin[a]

[a] *Department of Drug Metabolism, Merck Research Laboratories, Rahway, NJ, USA*
[b] *Department of Medicinal Chemistry, Merck Research Laboratories, Rahway, NJ, USA*

Received 19 August 2004; received in revised form 19 October 2004; accepted 28 October 2004
Available online 8 December 2004

Abstract

The compound, 5-{4-[3-(4-cyclohexyl-2-propylphenoxy)propoxy]phenyl}-1,3-oxazolidine-2,4-dione (compound **A**) is a peroxisome proliferator-activated receptor-γ (PPARγ) agonist. PPARγ agonists have proven useful in the treatment of type 2 diabetes, which is characterized by hyperglycemia, insulin resistance and/or abnormal insulin secretion. The metabolism of this oxazolidinedione (OZD) was investigated in male rat, dog, monkey and human liver microsomes, and recombinant human cytochrome P450 enzymes (CYP1A2, CYP2A6, CYP2B6, CYP2C8, CYP2C9, CYP2C19, CYP2D6, CYP2E1 and CYP3A4) in the presence of NADPH. Routes of metabolism included monohydroxylation of the cyclohexane ring at multiple positions, monohydroxylation of the *n*-propyl side chain or the tether linkage, and OZD ring opening, giving rise to the keto amide and alcohol amide entities. Liver microsomes showed subtle qualitative and quantitative metabolic differences among rat, dog, monkey and human preparations. Further, CYP2C8 and CYP2C19 did not display different regioselectivity for hydroxylation on the cyclohexane ring with both of them giving rise to C-3 and C-4 hydroxy metabolites, but they did display different stereoselectivity with CYP2C8 preferring cyclohexane hydroxylation in equatorial positions and CYP2C19 in axial positions.

Keywords: Compound **A**; 5-{4-[3-(4-Cyclohexyl-2-propylphenoxy)propoxy]phenyl}-1,3-oxazolidine-2,4-dione; Cytochrome P450 (CYP); Liquid chromatography (LC); Mass spectrometry (MS); Nuclear magnetic resonance (NMR); Peroxisome proliferator-activated receptor (PPAR)

1. Introduction

Diabetes mellitus is considered as one of the main threats to human health in the 21st century [1]. Indeed, the number of diabetics is expected to increase from approximately 151 million in the year 2000 to a potential total of 200–300 million cases in 2010 [2,3]. The most common form is type 2 diabetes, which is characterized by insulin resistance often in the presence of abnormal insulin secretion. Hyperglycemia may lead to nephropathy, neuropathy, retinopathy and atherosclerosis. Control of blood glucose levels may be achieved with oral hypoglycemic agents such as sulfonylureas, metformin, peroxisome proliferator-activated receptor-γ (PPARγ) agonists, α-glucosidase inhibitors and insulin [4]. Upon ligand binding, the nuclear hormone receptor PPARs regulate specific gene expression by binding to peroxisome proliferator responsive elements after heterodimerization with another nuclear receptor, the retinoid X receptor [5,6]. The PPARγ target genes are involved in the regulation of glucose and lipid metabolism. The ultimate outcome of administration of a PPARγ ago-

* Corresponding author. Present address: Department of Pharmacokinetics, Dynamics and Metabolism, Pfizer Global R&D, 2800 Plymouth Road, B25/330D Ann Arbor, MI 48105, USA. Tel.: +1 734 622 3547; fax: +1 734 622 4349.
E-mail address: arun.agrawal@pfizer.com (A.K. Agrawal).
[1] Present address: Department of Pharmacokinetics, Dynamics and Metabolism, Pfizer Global R&D, Eastern Point Road, MS8118-B3 Groton, CT 06340, USA.

0731-7085/$ – see front matter © 2004 Elsevier B.V. All rights reserved.
doi:10.1016/j.jpba.2004.10.036

nist is an increase in the sensitivity of certain tissues towards insulin, which enhances glucose metabolism and inhibits hepatic gluconeogenesis. Troglitazone, pioglitazone and rosiglitazone, all thiazolidinediones (TZDs), are PPARγ agonists and have shown clinical efficacy. However, troglitazone was withdrawn from the market because of idiosyncratic, but severe hepatotoxicity [7,8]. Subsequently, it has been shown that the TZD moiety of troglitazone was metabolically activated and gave rise to abundant glutathione adducts, which were detected in rat bile [9]. Although the relationship between TZD activation and hepatic toxicity remains unproven, oxazolidinediones (OZDs) were synthesized as PPARγ agonists in order to avoid this potential liability [10]. The in vitro metabolism of one of these is the subject of this report.

Detailed knowledge concerning the metabolism of potential drugs in preclinical species is required, because it must be established that the metabolites observed in humans were also present at appreciable concentrations in the species used for safety assessment [11]. In addition to liver microsomes from preclinical and clinical species, the ready availability of recombinant human cytochrome P450 enzymes has allowed for the identification of the isozyme(s) responsible for the metabolism of a compound [12]. In the present investigation, we have examined the in vitro metabolism of a new PPARγ OZD agonist: 5-{4-[3-(4-cyclohexyl-2-propylphenoxy)propoxy]phenyl}-1,3-oxazolidine-2,4-dione (compound **A**, Fig. 1) using LC–MS and ^{1}H NMR for structure elucidation of the metabolites. Subtle metabolic differences in the hydroxylation of this compound were observed when

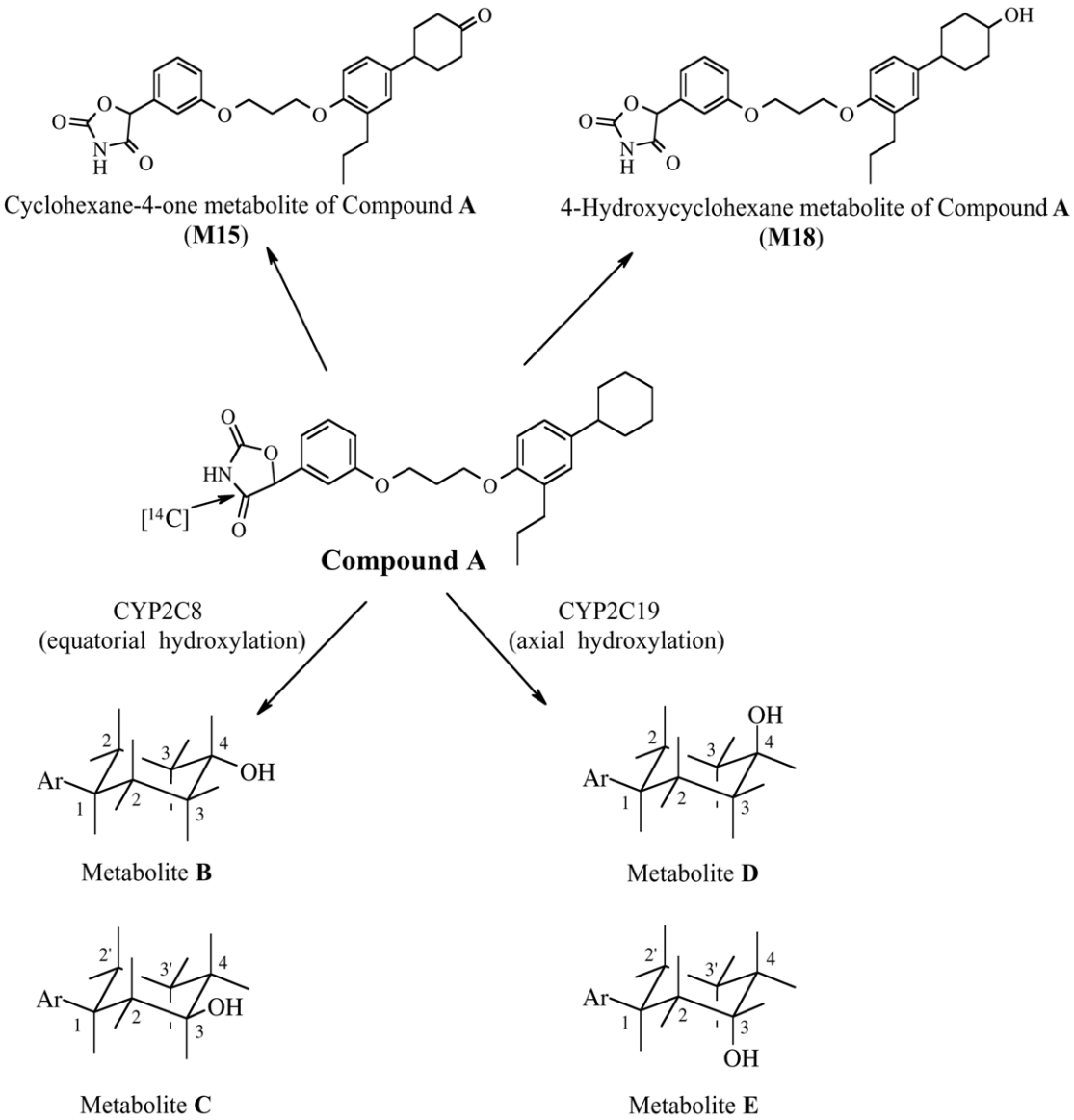

Fig. 1. Schematic presentation of [^{14}C]-compound **A**, and its oxidized and hydroxylated metabolites following incubation with CYP2C8 and CYP2C19. Procedural details are described under Section 2.

incubated with rat, dog, monkey and human liver microsomes and recombinant cytochrome P450 enzymes.

It is well known that drug metabolizing enzymes, such as cytochrome P450 enzymes, can display substrate and product stereoselectivity [13–15]. Data have been presented for the preferential metabolism of one enantiomer over the other for drugs administered as racemic mixtures. For example, CYP2B6 favored metabolism of *S*-methadone and CYP2C19 favored metabolism of *R*-methadone; CYP3A4 showed no preference [16]. In addition, formation of distinct enantiomers for prochiral drugs has been demonstrated. For example, the metabolism of the prochiral pesticide methoxychlor was studied using recombinant CYPs [17,18] and it was shown that CYP1A2 and CYP2A6 are biased towards formation of *R*-mono-OH methoxychlor via *O*-demethylation, whereas CYP1A1, CYP2B6, CYP2C8, CYP2C9, CYP2C19 and CYP2D6 preferentially form *S*-mono-OH methoxychlor; CYP3A4 and CYP3A5 did not display stereoselectivity. Data will be presented for the consistent but opposing stereochemical bias for hydroxylation of compound **A** on two adjacent carbon atoms by recombinant CYP2C8 and CYP2C19.

2. Materials and methods

Compound **A**, 5-{4-[3-(4-cyclohexyl-2-propylphenoxy)-propoxy]phenyl}-1,3-oxazolidine-2,4-dione, [^{14}C]-**A** and authentic standards of the 4-hydroxycyclohexane- and cyclohexane-4-one-metabolites of compound **A** (**M18** and **M15**, respectively; Fig. 1) were prepared at Merck Research Laboratories, Rahway, NJ, and their structures were confirmed by MS and ^{1}H NMR analyses. Male Sprague–Dawley rat, beagle dog, rhesus monkey and human liver microsomes were prepared by differential centrifugation [19]. The recombinant human P450 enzymes used were obtained from baculovirus-infected insect cells and were either prepared in-house or purchased from Gentest Corporation (Woburn, MA). All other chemicals were of analytical grade and solvents of HPLC grade.

2.1. Liver microsomal and recombinant CYP incubations

A or [^{14}C]-**A**, dissolved in methanol, was added to incubation media, such that the volume of methanol in the final incubation mixture was ≤1%. Incubations were carried out at 37 °C for 60 min in a shaking water bath. The incubation volume was 1 ml and consisted of 0.1 M potassium phosphate buffer (pH 7.4), magnesium chloride (1 mM), rat, dog, monkey or human liver microsomal protein (2 mg), **A** or [^{14}C]-**A** (50 μM) and NADPH (2 mM). Incubations that lacked NADPH served as negative controls. The incubations were terminated by the addition of an equal volume of acetonitrile, followed by centrifugation of the samples at 3000 rpm for 10 min at 4 °C. The supernatant was drawn off, evaporated to dryness under nitrogen gas, redissolved in 50% aqueous acetonitrile (200 μl), vortex-mixed and spun in a centrifuge at 3000 rpm for 10 min at 4 °C. The supernatant was transferred to a vial and placed in a Perkin Elmer Series 200 autosampler for analysis by LC–MS and LC–MS/MS. **A** and [^{14}C]-**A** were also incubated with microsomes prepared from baculovirus-infected cells expressing CYPs and cytochrome P450 reductase. Each incubation contained 50 μM **A** or [^{14}C]-**A** and 125 pmol of the individual CYP isoform (CYP1A2, CYP2A6, CYP2B6, CYP2C8, CYP2C9, CYP2C19, CYP2D6, CYP2E1 and CYP3A4) and was processed under identical conditions as described for liver microsomes.

2.2. LC–MS analysis

The metabolic profile of compound **A** was determined by reversed-phase HPLC analysis on a Zorbax XDB C-8 column (3.0 mm × 150 mm; 3.5 μm) using two Perkin Elmer Series 200 micro-LC pumps. Solvent A contained 1 mM ammonium acetate in water and solvent B contained acetonitrile + 1 mM ammonium acetate. The percentage of B increased from 20 to 80% in 30 min, followed by two minutes of isocratic conditions at 80% B. The flow rate was 0.5 ml/min of which 0.125 ml/min was directed to the mass spectrometer, and the remainder was either diverted to waste or collected in thirty second fractions for liquid scintillation counting (Beckman LS6500; Beckman Coulter Inc., Fullerton, CA). Mass spectral analysis was performed with a PE-Sciex API 3000 triple quadrupole mass spectrometer (Concord, Ont., Canada) using a Turbo Ionspray^{TM} interface operating in the positive or negative ionization mode. The MS and MS/MS conditions were optimized using compound **A**. Characterization of metabolites was achieved using collision-induced dissociation to obtain product ion mass spectra. The collision energy was 45 eV, the collision gas setting was at four and the temperature of the Turbo Ionspray^{TM} source was at 350 °C.

2.3. Bioreactor incubations

Compound **A** (50 μM) was incubated in a bioreactor with CYP2C8 or CYP2C19 expressing cells for the bulk production of metabolites [20]. The incubates were extracted with four volumes of ethyl acetate, the organic layer was separated and evaporated under vacuum in an evaporator. The residue was dissolved in mobile phase and the metabolites were isolated on a Zorbax Rx C-8 column. The eluent was collected in 1 min fractions. Based on the UV and MS responses, isolated fractions were selected for characterization by ^{1}H NMR.

2.4. NMR analysis

Compound **A** and the purified metabolites **B**–**E** (Fig. 1) were analyzed by ^{1}H NMR. The spectra were acquired in CD_3OD (0.13 ml) at 25°C (298 K) in 3 mm NMR tubes on a Varian Unity 400 MHz spectrometer using a Nalorac 3 mm indirect detection gradient probe (Varian Inc., Palo Alto, CA).

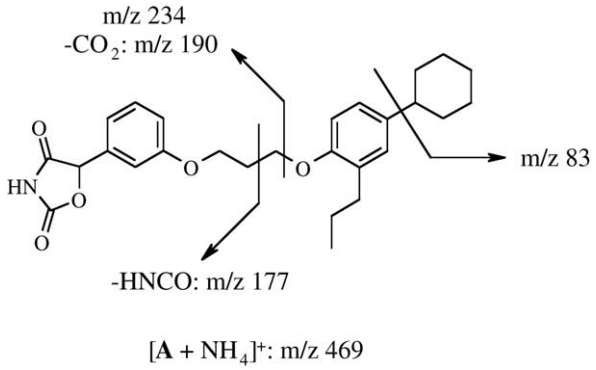

Fig. 2. Tentative structural assignments for the most informative fragmentation pathways observed for $[\mathbf{A} + NH_4]^+$ upon collision-induced dissociation.

The data processing was done on the spectrometer. Chemical shifts were reported on the δ scale (parts per million (ppm)) assigning the residual proton solvent peak to 3.30 ppm.

The 2D ^1H–^1H COSY (correlation spectroscopy) and NOESY (nuclear overhauser spectroscopy) spectra were acquired with a spectral width of 3198.2 Hz into 1 K data points in *f*2, and with 319 increments in the *f*1 dimension. The delays between successive pulses were 0.8 and 2.0 s for COSY and NOESY, respectively, and the 90° pulse was 7.75 μs. The mixing time was 400 ms for the NOESY spectra. The ^1H NOE (nuclear overhauser effect) difference spectra were acquired using a frequency list of one irradiation point (on-resonance) and one control (off-resonance) with a relaxation delay of 3.0 s. The difference spectrum was obtained by subtracting the control (off-resonance) from the other (on-resonance) for each irradiation point.

3. Results and discussion

3.1. MS and MS/MS data for compound *A*

Ionization of compound **A** in the negative mode gave rise to abundant *m*/*z* 450 ions ($[M - H]^-$). The product ion spectrum of compound **A** in the negative ionization mode was characterized by a very intense signal at *m*/*z* 42, which can be ascribed to $[NCO]^-$ from the OZD ring. The abundance of all other fragment ions (*m*/*z* 191, 203 and 217) was less than 5% of the intensity of the *m*/*z* 42 signal. Thus, little structural information could be obtained in the negative ionization mode. In the positive ionization mode, the $[M + H]^+$ signal at *m*/*z* 452 was relatively weak, but the $[M + NH_4]^+$ signal at *m*/*z* 469 was significantly more abundant. MS/MS fragmentation of the $[M + NH_4]^+$ ion of compound **A** gave rise to several structurally characteristic ions, including *m*/*z* 234, 190, 177 and 83; the assignment of the fragment ions is presented in Fig. 2. The intensity of *m*/*z* 83 ($[C_6H_{11}]^+$), albeit small, defined the cyclohexane ring. The product ion spectrum of the $[M + NH_4]^+$ ion from $[^{14}C]$-**A** was compatible with the assignments presented above for compound **A**.

The metabolites of compound **A** were identified by a three-step process:

I. identification of metabolites by LC–MS in the negative ionization mode;
II. confirmation of metabolites by LC–MS/MS in the negative ionization mode using *m*/*z* 42 precursor ion detection;
III. characterization of metabolites by LC–MS/MS in the positive ionization mode employing product ion scans of $[M + NH_4]^+$ and/or $[M + H]^+$.

3.2. Metabolism of compound *A* in rat, dog, monkey and human liver microsomes

$[^{14}C]$-**A** was incubated with rat, dog, monkey and human liver microsomes for 1 h at 37 °C in the absence or presence of NADPH. The turnover was higher in rat, monkey and human liver microsomes as compared to dog liver microsomes (data not shown). The LC–MS data indicated that the major metabolic pathways were oxidation of the cyclohexane ring (monohydroxylation, dihydroxylation and ketone formation). Other, mostly minor, metabolic processes included hydroxylation of the *n*-propyl side chain and the alkyl tether, as well as opening of the OZD ring (Fig. 3).

In the negative ionization mode, the extracted ion chromatograms for the $[^{14}C]$-$\mathbf{A} + O - H]^-$ ions at *m*/*z* 468 from rat, dog, monkey and human liver microsomal incubates exhibited subtle qualitative and quantitative differences in the types of hydroxylations occurring across the four species (see Fig. 4). In the positive ionization mode, the corresponding signals at *m*/*z* 470 ($[[^{14}C]$-$\mathbf{A} + H]^+$) were relatively weak. However, the intensities of the *m*/*z* 487 ($[[^{14}C]$-$\mathbf{A} + O + NH_4]^+$) and 452 ($[[^{14}C]$-$\mathbf{A} + O - H_2O + H]^+$) signals were significant. The greater abundance of the *m*/*z* 452 signals relative to those at *m*/*z* 470 indicated that the protonated hydroxy metabolites were relatively unstable and lost water in the ion source of the mass spectrometer. The latter observation indicated that hydroxylation of aliphatic carbon atoms, but not aromatic carbon atoms, had taken place. One of these metabolites was unambiguously identified; this hydroxylated metabolite co-eluted (retention time = 13.5 min) with an authentic standard of the 4-hydroxycyclohexane metabolite (**M18**, Figs. 1 and 3) and its product ion spectrum was also identical to that of the authentic standard. The positive ionization mode product ion spectrum of the ammonium adduct ions from the 4-hydroxycyclohexane metabolite exhibited characteristic signals at *m*/*z* 234, 190 and 81. Qualitatively, the spectrum was similar to that of the parent compound with the exception of the disappearance of *m*/*z* 83 and the appearance of *m*/*z* 81. The ion at *m*/*z* 81 corresponded with $[C_6H_{11} + O - H_2O]^+$, which was characteristic of hydroxylation of the cyclohexane ring.

The 4-hydroxycyclohexane metabolite was the predominant hydroxylated metabolite in human liver microsomes based on co-elution with the authentic standard of the

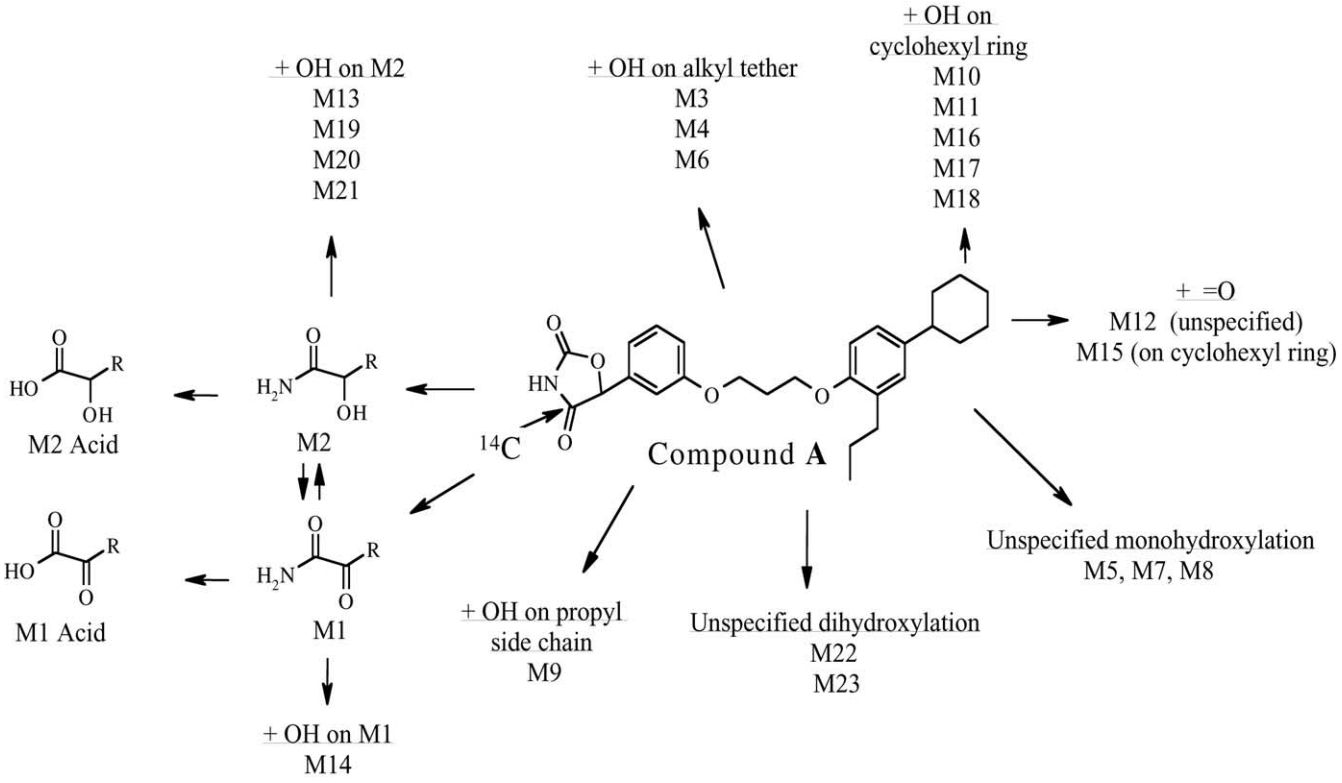

Fig. 3. Schematic presentation of in vitro metabolites produced following incubation of [^{14}C]-compound **A** with rat, dog, monkey and human liver microsomes, and recombinant cytochrome P450 isozymes (CYP2C8 and CYP2C19). M1–M23 = metabolites 1–23. Procedural details are described under Section 2.

4-hydroxycyclohexane metabolite, but this metabolite was less abundant in liver microsomes from rat, dog and monkey. Several hydroxylated metabolites of compound **A** had product ion spectra that were virtually identical to that of the 4-hydroxycyclohexane metabolite, which suggested that hydroxylation of the cyclohexane ring could occur at multiple positions. However, LC–MS/MS analyses could not provide definitive regioselective information regarding hydroxylation

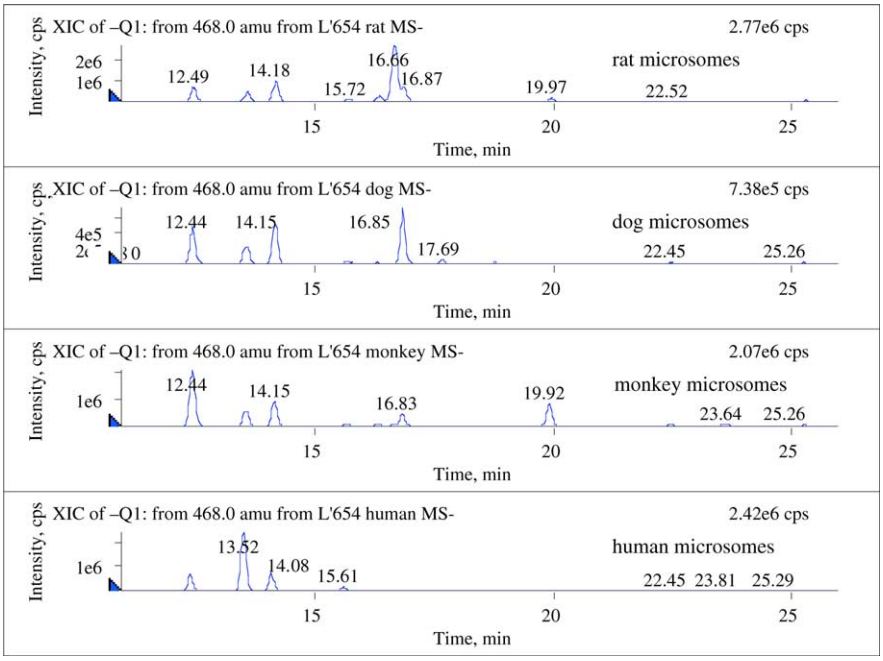

Fig. 4. Extracted ion chromatograms for the *m/z* 468 [[^{14}C]–**A** + O – H]$^-$ ions from compound [^{14}C]-**A** incubated with rat, dog, monkey and human liver.

of the cyclohexane ring. The tentative structural assignments of the various hydroxylated metabolites are presented in Fig. 3, based on their respective product ion spectra.

Relatively small quantities of compound **A** + 14 Da metabolites were detected as well. One of them was unambiguously identified because an authentic standard was available. This cyclohexane-4-one metabolite (**M15**, Figs. 1 and 3) gave rise to $[M+H]^+$ and $[M+NH_4]^+$ signals in the positive ionization mode. The product ion spectrum of the $[M+H]^+$ ions had a structurally characteristic ions at *m*/*z* 97 ($[C_6H_9O]^+$), which replaced *m*/*z* 83; this signal confirmed the presence of a ketone functionality on the cyclohexane ring.

The third, albeit minor, metabolic route for compound **A** was OZD ring opening, which has also been observed for thiazolidinediones [21–24]. Opening of the OZD ring, possibly initiated by hydroxylation of the tertiary carbon atom of the OZD ring or hydrolysis of the ester linkage, gave rise to the keto amide and alcohol amide entities (Fig. 3); both were further metabolized to the corresponding acids by amid hydrolysis.

3.3. Metabolism of compound *A* with recombinant cytochrome P450 enzymes

[^{14}C]-**A** was also incubated with recombinant CYP1A2, CYP2A6, CYP2B6, CYP2C8, CYP2C9, CYP2C19, CYP2D6, CYP2E1 and CYP3A4. The turnover was greatest with CYP2C8 followed by CYP2C19 and very little or no turnover was observed with the other CYPs (data not shown). The LC–MS data indicated that the major metabolic pathways were monohydroxylations and dihydroxylations.

Based on the similarity of the product ion mass spectra, it appeared that CYP2C8 and CYP2C19 generated, predominantly, hydroxylated cyclohexane metabolites. In contrast, incubation of compound **A** with CYP3A4 gave rise to a metabolite in which the hydroxy moiety was either associated with the *n*-propyl side chain or with the alkyl tether. However, product ion mass spectra could not differentiate between the two possibilities.

3.4. NMR analysis

To obtain more information about the regiochemistry and stereochemistry of the hydroxylated metabolites, compound **A** was incubated in a bioreactor with the cytochrome P450 expressing cells which had the most turnover, i.e. CYP2C8 and CYP2C19, followed by isolation of the most abundant metabolites and analysis by ^{1}H NMR. NMR assignments were made on the basis of ^{1}H chemical shifts, ^{1}H–^{1}H couplings (Table 1) together with 1D NOE, COSY and NOESY correlations.

^{1}H NMR analysis was conducted on the synthetic standard of compound **A** (Table 1). The aromatic region of the ^{1}H NMR spectrum of compound **A** indicated two aromatic systems, one 1,3-disubstituted (7.25 and 6.95–6.87 ppm) and one 1,2,4-trisubstituted (6.95–6.87 and 6.80 ppm). The aliphatic region showed the presence of a low field proton (5.38 ppm) from the 2,4-oxazolidinedione ring, a 1,3-propyl diether moiety (4.19, 4.11 and 2.22 ppm), an *n*-propyl group (2.53, 1.54 and 0.87 ppm) and a monosubstituted cyclohexane ring (2.38, 1.81, 1.73, 1.38 and 1.28 ppm). The splitting pattern of the proton at position 1 of the cyclohexane ring and its NOE connectivities with the axial protons at position 3 (data not shown) indicated that the proton at position 1 was axial.

NMR analysis of the two chromatographic fractions containing metabolites **B** and **C**, isolated from the incubation of compound **A** with CYP2C8, indicated that the hydroxylation occurred in the cyclohexane ring (Fig. 1 and Table 1). (The fractions containing metabolites **B** and **C** correspond with the signals at 13.5 and 14.1 min in Fig. 4, respectively.) Both fractions had H-1 in the axial position, as discerned from the large coupling constants (11.8 and 12.1 for **B** and **C**, respectively). The fraction containing metabolite **B** showed symmetry of the cyclohexyl proton signals, suggesting that the hydroxyl group was located at C-4. The proton at position 4 was displaced downfield (3.58 ppm) and showed one large coupling constant (10.7 Hz) which was diagnostic of an axial configuration. The NOESY experiment showed NOE connectivities for H-4 with H-3 equatorial and H-2 axial, confirming that H-4 was axial, which meant that the hydroxyl group was equatorial. The fraction containing metabolite **C** showed the loss of symmetry in the cyclohexyl proton signals which limited the choice to the C-2 or C-3 sites for the hydroxylation. The proton of the cyclohexane ring most displaced downfield (3.62 ppm) showed a large coupling constant (11.0 Hz) diagnostic of an axial configuration. 1D NOE and NOESY experiments showed NOE connectivities for this proton with H-4 equatorial, H-3′ axial, H-2 equatorial and H-1 axial, confirming that this proton was at the axial C-3 position, which meant that the hydroxyl group was equatorial.

NMR analysis of the chromatographic fraction isolated from the incubation of compound **A** with CYP2C19 indicated the presence of two hydroxylated metabolites, **D** and **E**, with the hydroxyl moiety in the cyclohexane ring with a ratio of 2:1, respectively (Fig. 1 and Table 1). (The fractions containing metabolites **D** and **E** correspond with the signals at 13.5 and 14.1 min in Fig. 4, respectively.) An axial H-1 in both metabolites was indicated by the large coupling constants, 11.7 and 12.1 Hz for **D** and **E**, respectively. The major component, metabolite **D**, showed symmetry of the cyclohexane proton signals suggesting that the hydroxyl group was located at C-4. The proton at position 4 was displaced downfield (4.00 ppm) and, due to the absence of a large axial–axial coupling constant, the configuration of the hydroxyl substituent was determined to be axial. The NOESY experiment showed NOE connectivities for H-4 with H-3 equatorial and H-3 axial, confirming that the H-4 was equatorial. The minor component, metabolite **E**, also showed an axial hydroxyl substituent, but its location was limited to the C-2 or C-3 positions because of the loss of symmetry in the cyclohexane proton signals. Of these two possibilities, the

Table 1
^{1}H NMR chemical shifts (ppm) assignments for compound **A** and its cyclohexyl hydroxy metabolites **B**–**E**

Proton(s)	Compound **A**	CYP2C8 (OH equatorial)		CYP2C19 (OH axial)	
		Metabolite **B**	Metabolite **C**	Metabolite **D**	Metabolite **E**
	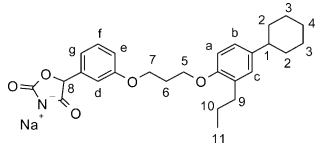	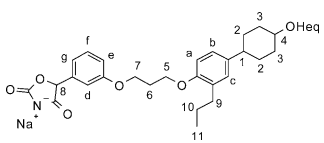	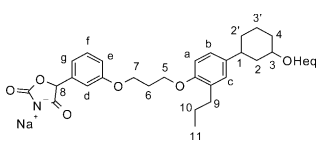	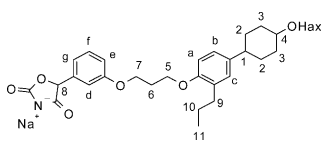	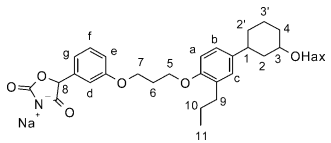
H-f	7.25 (t, 1H, *J* = 8.1 Hz)	7.27 (t, 1H, *J* = 8.1 Hz)	7.30 (t, 1H, *J* = 8.3 Hz)	7.32 (t, 1H, *J* = 8.0 Hz)	7.32 (t, 1H, *J* = 8.0 Hz)
H-b,c,d,e,g	6.95–6.87 (m, 5H)	6.96–6.89 (m, 5H)	6.97–6.92 (m, 5H)	6.99–6.93 (m, 5H)	6.99–6.93 (m, 5H)
H-a	6.80 (d, 1H, *J* = 8.4 Hz)	6.81 (d, 1H, *J* = 8.3 Hz)	6.83 (d, 1H. *J* = 8.3 Hz)	6.82 (d, 1H, *J* = 8.2 Hz)	6.82 (d, 1H, *J* = 8.2 Hz)
H-8	5.38 (s, 1H)	5.47 (s, 1H)	5.65 (s, 1H)	5.75 (s, 1H)	5.75 (s, 1H)
H-7	4.19 (t, 2H, *J* = 6.1 Hz)	4.19 (t, 2H, *J* = 6.1 Hz)	4.20 (t, 2H, *J* = 6.1 Hz)	4.21 (t, 2H, *J* = 6.1 Hz)	4.21 (t, 2H, *J* = 6.1 Hz)
H-5	4.11 (t, 2H, *J* = 6.1 Hz)	4.12 (t, 2H, *J* = 6.1 Hz)	4.13 (t, 2H, *J* = 6.1 Hz)	4.13 (t, 2H, *J* = 6.1 Hz)	4.13 (t, 2H, *J* = 6.1 Hz)
H-9	2.53 (t, 2H, *J* = 7.6 Hz)	2.53 (t, 2H, *J* = 7.6 Hz)	2.54 (t, 2H, *J* = 7.6 Hz)	2.54 (t, 2H, *J* = 7.5 Hz)	2.54 (t, 2H, *J* = 7.5 Hz)
H-6	2.22 (quintet, 2H, *J* = 6.1 Hz)	2.23 (quintet, 2H, *J* = 6.1 Hz)	2.24 (quintet, 2H *J* = 6.1 Hz)	2.24 (quintet, 2H, *J* = 6.1 Hz)	2.24 (quintet, 2H, *J* = 6.1 Hz)
H-10	1.54 (sextet, 2H, *J* = 7.5 Hz)	1.53 (sextet, 2H, *J* = 7.5 Hz)	1.54 (sextet, 2H, *J* = 7.4 Hz)	1.55 (m, 2H)	1.55 (m, 2H)
H-11	0.87 (t, 3H, *J* = 7.5 Hz)	0.87 (t, 3H, *J* = 7.3 Hz)	0.87 (t, 3H, *J* = 7.4 Hz)	0.87 (t, 3H, *J* = 7.4 Hz)	0.87 (t, 3H, *J* = 7.4 Hz)
H-4eq	1.73 (bd, 1H, *J* = 12.5 Hz)		1.98 (bd, 1H, *J* = 11.4 Hz)	4.00 (t, 1H, *J* = 2.7 Hz)	1.87 (m, 1H)
H-4ax	1.28 (m, 1H)	3.58 (tt, 1H, *J* = 4.2, 10.7 Hz)	1.23 (m, 1H)		1.51 (m, 1H)
H-3eq	1.81 (m, 2H)	2.02 (bd, 2H, *J* = 11.7 Hz)		1.85 (m, 2H)	4.11 (m, 1H)
H-3ax	1.38 (m, 2H)	1.39 (m, 2H)	3.62 (tt, 1H, *J* = 4.2, 11.0 Hz)	1.63 (m, 2H)	
H-3′eq			1.85 (dt, 1H, *J* = 3.3, 13.3 Hz)		1.87 (m, 1H)
H-3′ax			1.41 (tt, 1H, *J* = 3.4, 13.2 Hz)		1.79 (m, 1H)
H-2eq	1.81 (m, 2H)	1.83 (bd, 2H, *J* = 12.2 Hz)	2.04 (bd, 1H, *J* = 11.5 Hz)	1.85 (m, 2H)	1.87 (m, 1H)
H-2ax	1.38 (m, 2H)	1.48 (m, 2H)	1.29 (m, 1H)	1.52 (m, 2H)	1.56 (m, 1H)
H-2′eq			1.73 (bd, 1H, *J* = 13.0 Hz)		1.87 (m, 1H)
H-2′ax			1.26 (m, 1H)		1.44 (m, 1H)
H-1ax	2.38 (m,1H)	2.38 (tt, 1H, *J* = 3.4, 11.8 Hz)	2.48 (tt, 1H, *J* = 3.2, 12.1 Hz)	2.43 (tt, 1H, *J* = 3.3, 11.7 Hz)	2.89 (tt, 1H, *J* = 3.3, 12.1 Hz)

Signal splitting patterns: s = singlet, d = doublet, bd = broad doublet, *t* = triplet, dt = doublet of triplet, tt = triplet of triplets, m = multiplet.

C-3 site was the only choice since the coupling pattern of the C-1 proton indicated that no substitution had occurred on either of the neighboring carbons. This assignment was also consistent with the NOESY and an NOE experiment in which irradiating H-1 produced NOE signals from the equatorial and axial C-2 and C-2′ protons.

4. Conclusions

In conclusion, the in vitro metabolism of a PPARγ agonist, 5-{4-[3-(4-cyclohexyl-2-propylphenoxy)propoxy]phenyl}-1,3-oxazolidine-2,4-dione (compound **A**) was investigated in liver microsomes from rats, dogs, monkeys and humans, and recombinant human CYPs. Mass spectral evidence indicated that oxidation of the cyclohexane ring was the major metabolic pathway; minor pathways included hydroxylation of the alkyl tether and the *n*-propyl substituent and ring opening of the OZD ring, giving rise to the keto amide and alcohol amide entities. Metabolism by CYP2C8 gave rise to hydroxylated metabolites where the hydroxy entities were in the cyclohexane ring at carbons 3 and 4 and occupied equatorial positions, as concluded from the ^{1}H NMR studies. On the other hand, metabolism by CYP2C19 also gave rise to hydroxylated metabolites in the cyclohexane ring at carbons 3 and 4, but the hydroxy entities were in the axial positions. Thus, CYP2C8 and CYP2C19 did not display different regioselectivity for hydroxylation on the cyclohexane ring, but they did display different stereoselectivity with CYP2C8 preferring cyclohexane hydroxylation in equatorial positions and CYP2C19 in axial positions.

Acknowledgments

We would like to express our thanks to Drs. T. Rushmore and M. Shou for their work with the bioreactors and to Mr. B. Cato and Dr. D. Dean for the synthesis of the radiolabeled compound, [^{14}C]-**A**. Also, our sincere thanks go to Drs. H. Koyama and S. Sahoo for supplying compound **A** and authentic standards of metabolites.

References

[1] P. Zimmet, K.G.M.M. Alberti, J. Shaw, Nature 414 (2001) 782–787.
[2] A.F. Amos, D.J. McCarty, P. Zimmet, Diabet. Med. 14 (Suppl. 5) (1997) S1–S85.
[3] P.G. Kopelman, G.A. Hitman, Diabet. Lancet 352 (Suppl. 4) (1998) SIV5.
[4] D.E. Moller, Nature 414 (2001) 821–827.
[5] A.B. Jones, Med. Chem. Rev. 21 (2001) 540–552.
[6] J. Berger, D.E. Moller, Annu. Rev. Med. 53 (2002) 409–435.
[7] N. Gitlin, N.L. Julie, C.L. Spurr, K.N. Lim, H.M. Jurabe, Ann. Int. Med. 129 (1998) 38–41.
[8] B.A. Neuschwander-Tetri, W.L. Isley, J.C. Oki, S. Ramrakhini, S.G. Quiason, N.J. Phillips, E.M. Brunt, Ann. Int. Med. 129 (1998) 36–38.
[9] K. Kassahun, P.G. Pearson, W. Tang, I. McIntosh, K. Leung, C. Elmore, D. Dean, R. Wang, G. Doss, T.A. Baillie, Chem. Res. Toxicol. 14 (2001) 62–70.
[10] R.C. Desai, D.F. Gratale, W. Han, H. Koyama, E. Metzger, V.K. Lombardo, K.L. MacNaul, T.W. Doebber, J.B. Berger, K. Leung, R. Franklin, D.E. Moller, J.V. Heck, S.P. Sahoo, Bioorg. Med. Chem. Lett. 13 (2003) 3541–3544.
[11] T.A. Baillie, M.N. Cayen, H. Fauda, R.J. Gerson, J.D. Green, S.J. Grossman, L.J. Klunk, B. LeBlanc, D.G. Perkins, L.A. Shipley, Toxicol. Appl. Pharmacol. 182 (2002) 188–196.
[12] V. Subrahmanyan, A.B. Renwick, D.G. Walters, P.J. Young, R.J. Price, A.P. Tonelli, B.G. Lake, Drug Metab. Dispos. 29 (2001) 1146–1155.
[13] W.F. Trager, Drug Metab. Rev. 20 (1989) 489–496.
[14] B. Testa, The Metabolism of Drugs and Other Xenobiotics, Academic Press, London, UK, 1995.
[15] D.R. Brocks, F. Jamali, Pharmacotherapy 15 (1995) 551–564.
[16] J.G. Gerber, R.J. Rhodes, J. Gal, Chirality 16 (2004) 36–44.
[17] Y. Hu, D. Kupfer, Drug Metab. Dispos. 30 (2002) 1329–1336.
[18] Y. Hu, K. Krausz, H.V. Gelboin, D. Kupfer, Xenobiotica 34 (2004) 117–132.
[19] J.L. Raucy, J.M. Lasker, in: M.R. Waterman, E.F. Johnson (Eds.), Methods in Enzymology, vol. 206, Academic Press, San Diego, CA, 1991, pp. 557–587.
[20] T.H. Rushmore, P.J. Reider, D. Slaughter, C. Assang, M. Shou, Metab. Eng. 2 (2000) 115–125.
[21] H.G. Fouda, J. Lukaszewicz, D.A. Clark, B. Hulin, Xenobiotica 21 (1991) 925–934.
[22] P.A. Krieter, A.E. Colletti, G.A. Doss, R.R. Miller, Drug Metab. Dispos. 22 (1994) 625–630.
[23] Y. Kiyota, T. Kondo, Y. Maeshiba, A. Hashimoto, K. Yamashita, Y. Yoshimura, M. Motohashi, S. Tanayama, Arzneim-Forsch/Drug Res. 47 (1997) 22–28.
[24] P.J. Cox, D.A. Ryan, F.J. Hollis, A.-M. Harris, A.K. Miller, M. Vousden, H. Cowley, Drug Metab. Dispos. 28 (2000) 772–780.